Introduction

Phosphorus can exist in two allotropes: black phosphorus (BP) and white phosphorus (WP). Whether phosphorus crystallises to BP or WP depends on thermodynamics. The difference in crystal structure between black and WP is due to the different arrangement of the phosphorus atoms, which leads to differences in stability, reactivity, and density.

WP has a tetrahedral arrangement of atoms with each atom bonded to three others in a planar arrangement. The α form is defined as the standard state of the element, but is actually metastable under standard conditions. It has a body-centred cubic crystal structure, and transforms reversibly into the β form at 195.2 K. The β form is believed to have a hexagonal crystal structure. This structure is less compact and more reactive than BP, and it has a lower density. WP is also a highly reactive and flammable material, and it will ignite spontaneously in air at about 30°C. WP is typically used to manufacture chemicals used in fertilisers, food additives, and cleaning compounds. WP is also used by the military in ammunition as an incendiary agent due to its spontaneous combustibility. [1]

BP was first synthesised by heating WP under high pressures (12,000 atmospheres) in 1914. The applications of BP extends to field effect transistors, rechargeable batteries, electrocatalysis, sensors, thermoelectric materials etc. BP is a layered material with a puckered, hexagonal arrangement of atoms, resulting in a more compact structure compared to WP. BP has an orthorhombic pleated honeycomb structure and is the least reactive allotrope due to its lattice of interlinked six-membered rings with each atom (5 outer shell electrons) bonded to three other atoms.

In this report, structural parameters such as the bulk modulus are predicted and electronic properties such as the electron energy loss spectra (EELS), density of states (DOS), partial DOS (PDOS) and band structures are also studied.

Methodology

CASTEP is a density-functional theory (DFT) based code for studying a wide range of materials and systems. By supplying the vectors that define the lattice and the atoms in the unit cell. The electrons are treated as independent and the exchange correlation functionals only depend on the electron density.

For speedup, the MPI run command is used for parallelisation. A kpoint based on the sampling of the Brillouin zone convergence was carried out and the PDOS were analysed to determine the suitability of different kpoint grids. By iteratively, solving the self-consistent field, the ground state can be determined. Many materials properties are predicted as functionals of the energy density. Firstly, the desired lattice parameter, atomic positions and other calculation parameters are specified. Initially, single point energy calculations are used to calculate the total energy of a system. Geometry optimisation is carried out, saving the geometry optimised structure for band structure calculations.

Exchange correlation functionals are used to capture electronic behaviour between the electrons. LDA (Local Density Approximation) and PBE (Perdew-Burke-Ernzerhof) are both commonly used. In general, LDA tends to overbind, meaning that it predicts that the total energy of a system is lower (more stable) than what it actually is. This results in the LDA calculated bond lengths and binding energies being too short and too strong, respectively. On the other hand, PBE is known to underbind, meaning that it predicts that the total energy of a system is higher (less stable) than what it actually is. This results in the PBE calculated bond lengths and binding energies being too long and too weak, respectively. While both LDA and PBE are widely used, each has its own strengths and limitations. For example, LDA is computationally less expensive and can be used to quickly obtain rough estimates of properties, but it may not provide accurate predictions for certain materials. PBE, on the other hand, is more accurate, but is also more computationally expensive. Ultimately, the choice of XC functional depends on the specific material or system being studied

and the level of accuracy required. In some cases, a hybrid functional that combines the strengths of both LDA and PBE may be used. Both LDA and PBE converged quickly for BP. However, even after over 2.5 hours running a Geometry Optimisation for WP using PBE and it did not converge. As such, only LDA calculations were used for WP.

The DOS of a system describes the proportion of states that are to be occupied by the system at each energy. The PDOS is the projection of a particular orbital of a particular atom on the DOS. As such, summing over all the projections, returns the DOS.

The k-point path is specified for the band structure calculation of a system. After the calculation, the band structure can be visualised. EELS (Electron Energy-Loss Spectroscopy) calculations in CASTEP are run in CASTEP by specifying the desired energy loss range and the spectral k-point grid used was usually 16 16 16.

The bulk modulus of a system was calculated by applying a hydrostatic pressure to the system and running a geometry optimisation, noting the volume and using the EXCEL linest function to find the slope. The product of the reciprocal of the slope and the equilibrium volume is the bulk modulus.

The individual P4 molecule for WP and monolayer BP structures were created by manipulating the structure in VESTA. The conversion to cartesian coordinates for monolayer BP was to make spanning through the monolayer simple in CASTEP.

Results

WP

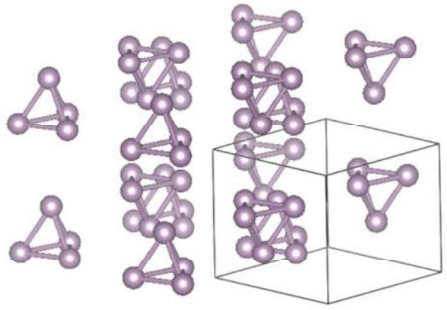

Figure 1: WP Structure after Geometry optimisation (VESTA)

White Phosphorus						
Functional	Lattice Parameters			Cell Angles		
	a	b	c	Alpha	Beta	Gamma
LDA	5.8232	5.832	5.187	90.34	90.34	82.51
PBE 1	7.028549	7.028549	6.137	90.783	90.783	83.215
PBE 2	6.973787	6.973787	6.093029	90.759064	90.759064	83.264464
PBE 3	7.083398	7.083398	6.177436	90.807383	90.807383	83.170368
PBE 4	7.1731752	7.131752	6.215336	90.831316	90.831316	83.13547

Table 1: WP lattice parameters and cell angles

For WP, the geometry optimisation (geom op) for PBE did not converge, even after over 2 hours. The PBE runs simply stopped after 30 cycles. However, by analysing just the PBE runs, it is clear that the lattice parameters and cell angles a, b, c, α, β and γ would converge around 7.1, 7.1, 6.1, 90.8, 90.8 and 83.1. There is a significant difference in the lattice parameters for the LDA and the 4 PBE runs that did not converge. For the rest of the report, LDA values are used for electronic calculations. For more accurate calculations, a XC that produces a structure between that produced by LDA and PBE should be used to negate the significant under and over binding observed in Table 1.

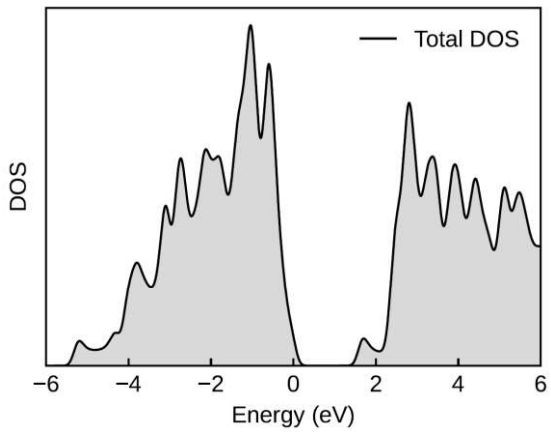

Figure 2: LDA DOS

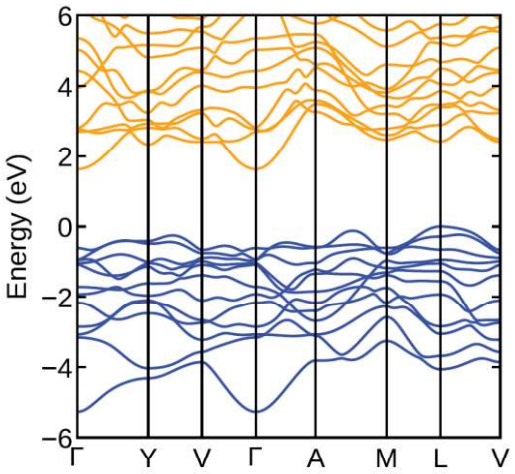

Figure 3: LDA band structure

From reading through the band.dat file, the bandgap is 1.62eV. The bandgap is also apparent from the DOS.

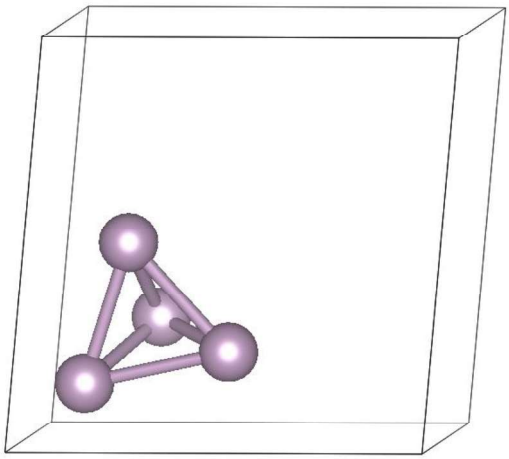

Figure 4: Optimised structure for P4 molecule (VESTA)

White Phosphorus P4						
Functional	Lattice Parameters			Cell Angles		
	a	b	c	Alpha	Beta	Gamma
LDA	6.2	6.2	5.43	90.23	90.23	84.56

Table 2: Optimised structure for P4 molecule

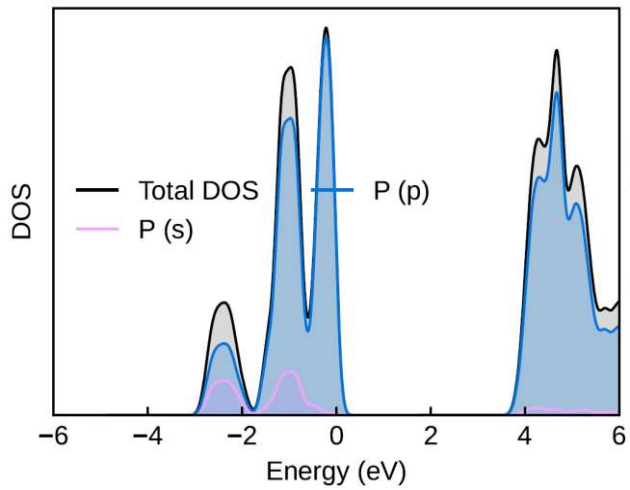

Figure 5: LDA PDOS single structure

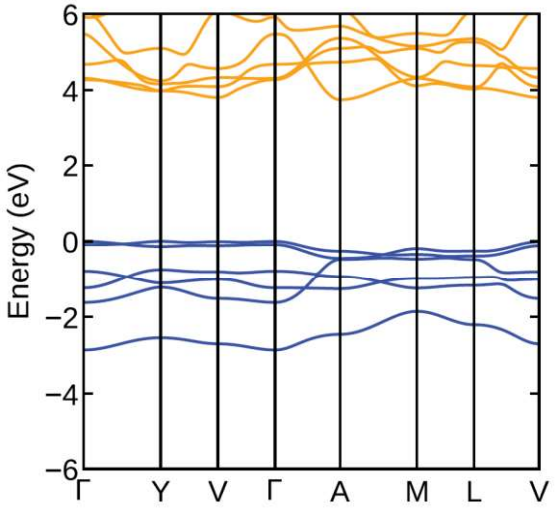

Figure 6: LDA band structure single structure

From reading through the band.dat file, the bandgap of 3.8eV which is greater than 1.62eV for the bulk structure. BP PDOS is electrically conductive. Mostly p character.

BP

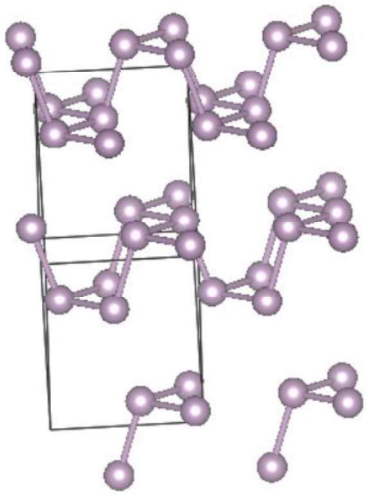

Figure 7: BP after Geometry Optimisation (VESTA)

Black Phosphorus						
Functional	Lattice Parameters			Cell Angles		
	a	b	c	Alpha	Beta	Gamma
LDA 4 4 4	5.409035	5.409035	3.734944	90	90	143.715547
LDA 6 6 6	5.494509	5.494509	4.37536	90	90	144.89569
LDA 8 8 8	5.36434	5.36434	4.091672	90	90	143.934355
PBE 4 4 4	5.943138	5.943138	4.50758	90	90	147.270008

Table 3: BP lattice parameters and cell angles

There is not much of a difference between the lattice parameters and cell angles of BP. The LDA optimised structure was used for the rest of the calculations.

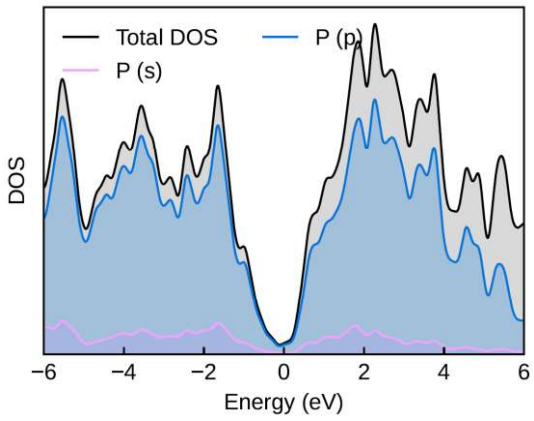

Figure 8: LDA PDOS before geom op 4 4 4

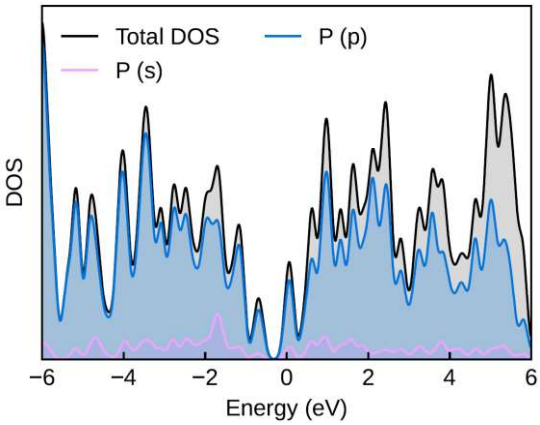

Figure 9: LDA PDOS after geom op 4 4 4

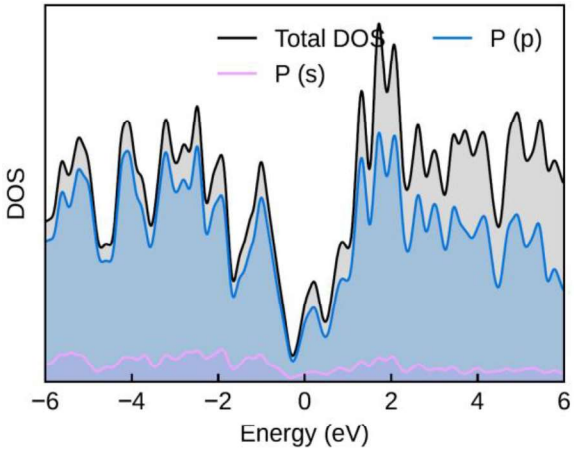

Figure 10: LDA PDOS after geom op 8 8 8

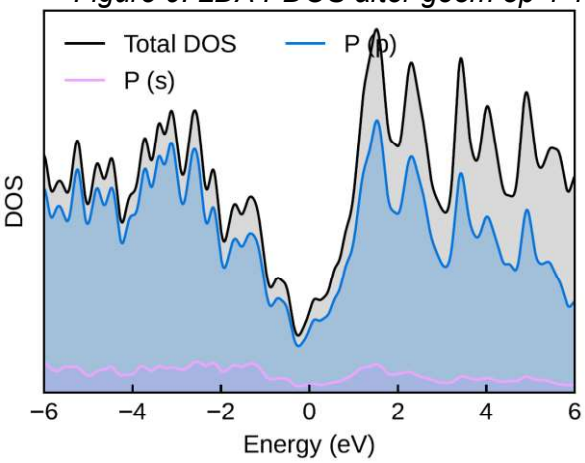

Figure 11: LDA PDOS after geom op 12 12 12

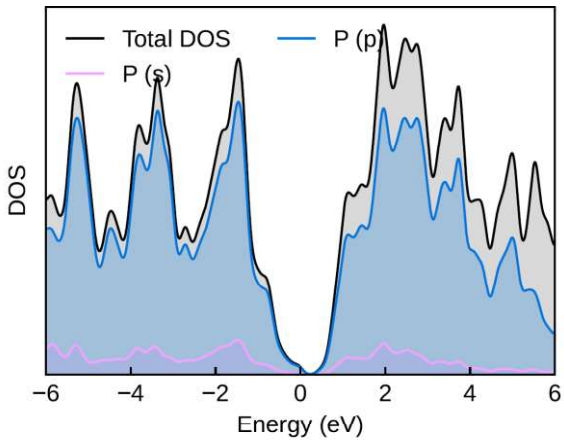

Figure 12: PBE PDOS after geom op 4 4 4

Comparing the PDOS before and after geometry optimisations for a kpoint grid of 4 4 4, there are many more peaks. The most important feature being the size and position of the trough still remains the same through all the kpoints grids. It is apparent that the LDA has the trough at a lower energy than PBE. This mirrors the underbinding and overbinding character of the XC functionals.

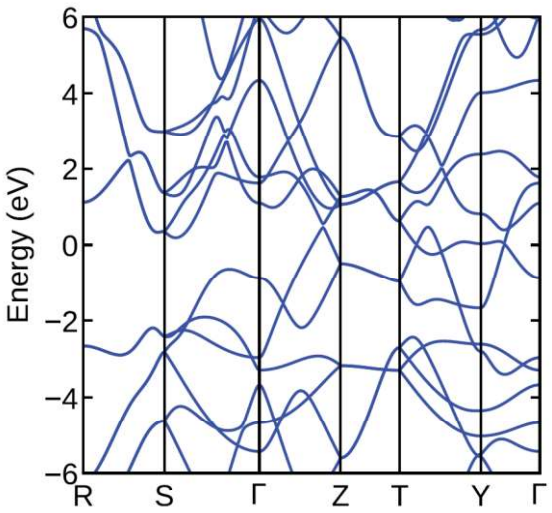

Figure 13: LDA band structure

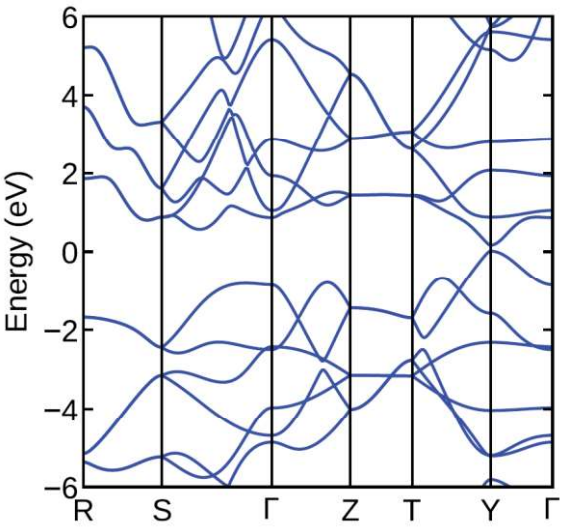

Figure 14: PBE band structure

The band structures from both XC functionals display metallic behaviour without any band gap.

dp/dv	-1.4E+39	Eqm V A**3	64.66878
Bulk Modulus	9.1E+10	Eqm V	6.47E-29

Table 4: BP bulk

dp/dv	-4.7E+38	Eqm V A**3	148.1583
Bulk Modulus	7E+10	Eqm V	1.48E-28

Table 5: BP monolayer

The bulk modulus for bulk and monolayer BP is 91 GPa and 70 GPa respectively.

Black Phosphorus Monolayer						
Functional	Lattice Parameters			Cell Angles		
	a	b	c	Alpha	Beta	Gamma
LDA	3.27	10.48	4.32	90	90	90

Table 6: Optimised structure for BP monolayer

The cell file was created in cartesian coordinates to have the layer span the planes of the lattice parameters in a and c and set up to use the minimum cell size that contains a single layer while allowing the cell to be propagated in the a and c directions.

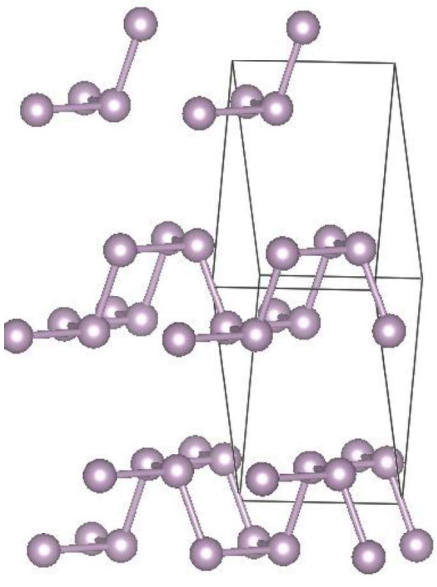

Figure 15: bulk structure (VESTA)

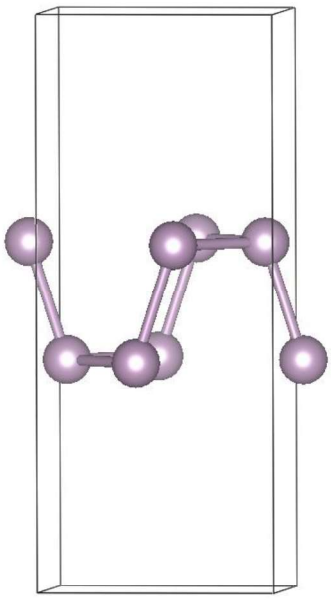

Figure 16: Monolayer structure (VESTA)

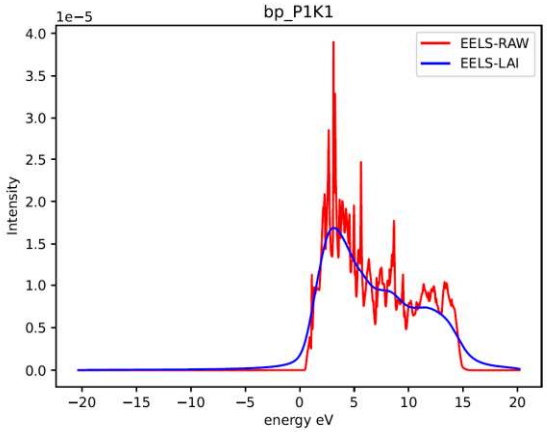

Figure 17: EELS P1K1

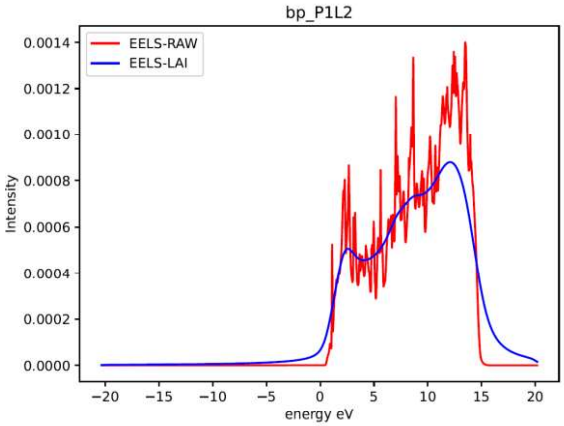

Figure 18: EELS P1L2

Only EELS diagrams for BP were calculated. The EELS for all 1st shells (i.e K1 and L1) have the same features. Similarly, all second shells (i.e K2 and L2) graphs also look the same. This is due to the structure of the electronic shells within the atoms. The EELS resembles that of the literature and allows for the distinguishing between WP and BP allotropes, important to any experimental studies on the crystallisation of each and whether any oxidation took place.

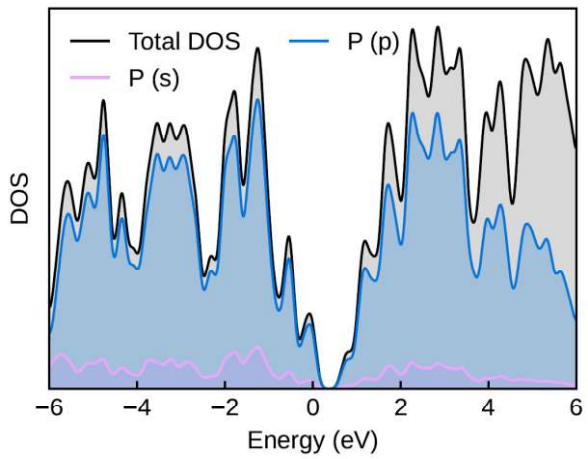

Figure 19: PDOS monolayer

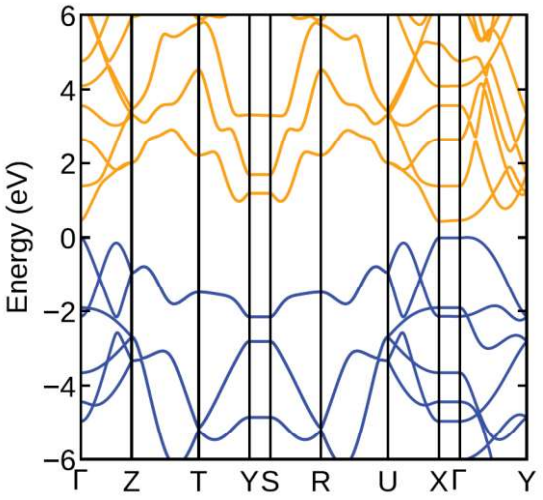

Figure 20: monolayer band structure

From reading through the band.dat file, the band gap of 0.43eV

Most of the character of the bonds in BP is from the p orbitals. The overlap in the monolayer produces graphene-like electrical properties. Compared to literature the PDOS.

Discussion

During the geometry optimisations, there were much greater variations in the lattice parameters than the cell angles. This is likely due to an optimisation of distance between atoms due to isotropic stresses rather than any in plane anisotropic stresses or strains. The failed convergence of the WP for PBE is due to the limit set by the 30 cycles. Although it still did not converge when the limit was set to 60. The high number of cycles required would not be a problem for a more parallelised system with many more computing cores.

WP is an indirect bandgap semiconductor with a bandgap of typically between 1.5-2.0 eV [2] and 1.62eV from the calculations. Unlike BP, from figure 1 and 4, the structure of the P4 molecules results in WP being a not a highly anisotropic material, and its conductivity is isotropic in all directions. The individual P4 molecule is predicted to have a much greater band gap of 3.8 eV compared to 1.62 eV. This is likely due to the individual P4 molecule being much less strained than

the bulk form. This is true in GaX monolayers where increasing tensile strain decreases the band gap. [3] It could be argued that the orientation of the band structure calculation also affected the band gap but the nature of the calculation is to plot along paths between high symmetry points. By comparing figure 3 and 6, it is observed that the number of lines in each band varies significantly. This is due to the fewer paths that are through high symmetry points for a single P4 molecule. Similar is true of the PDOS, in figures 2 and 5, where there are fewer peaks in the PDOS for the single P4 molecule.

It is evident from the band structure calculations that the properties of bulk WP do not change significantly from the individual P4 molecules. As such, the tuning of bulk WP is highly dependent on the individual P4 molecules.

The similarity of the lattice parameters for both the LDA and PBE runs suggest that. LDA geometry optimisation was run with different kpoint grids from 4 4 4, 6 6 6 and 8 8 8. They all displayed similar lattice parameters without a clear increasing or decreasing trend. As such, it is likely that the lattice parameters oscillate closely around the true structure. Given the small around 1% changes between the lattice parameters, a 4 4 4 kpoint grid is suitable.

In comparison to graphite and graphene, monolayer BP (phosphorene) has a non-zero bandgap. The band gap can be tuned by strain and stacking different numbers of layers together. Contrary to my calculations, there is evidence in literature that bulk phosphorene has a 0.3 eV. [4] Increase in band gap value in single-layer phosphorene is predicted to be caused by the absence of interlayer hybridization near the top of the valence and bottom of the conduction band. [5] Both LDA and PBE displayed metallic behaviour for bulk BP.

BP's unique topological structure and differences between the armchair (AM) and zigzag (ZZ) directions, phosphorene displays strong in-plane anisotropy with many properties in these two principal directions drastically different. As the valence band is dominated by p-orbitals, while the conduction band is primarily made up of s-orbitals, the directionality of the p-orbitals dominance as seen in the PDOS in figure 19 makes BP a highly anisotropic material, with strong in-plane conductivity and weak out-of-plane conductivity.

The difference in the bulk modulus of bulk and monolayer BP in table 4 and 5 is not large. It could be due to the different ways the cell is structured as seen in figure 15 and 16 from non-cartesian to cartesian. Importantly, it is evident the stress exerted is taken up by the bonds between phosphorus atoms instead of on the Van Der Waals forces between the layers. Graphene has a bulk modulus of 97.5 GPa compared to the predicted 70GPa for monolayer BP. As such, many of the structures that graphene for which graphene has been considered should also consider monolayer BP. It is possible that monolayer BP would be useful for computing devices due to its semiconducting properties and easy production via exfoliation.

White phosphorus is incredibly harmful. White phosphorus burns in air and causes severe burns upon contact with skin or eyes. White phosphorus smoke will also cause eye and respiratory tract irritation. Other initial adverse health effects are primarily due to gastrointestinal irritation. [1] When carrying out experimental work, the experimental EELS spectra can be compared with the theoretical versions to determine the type of allotrope purity, degree of oxidation, distance between layers. It can be observed as additional peaks and or changes in the shape of the curves. Detection systems can be run to determine the presence of white phosphorus during manufacturing processes for fertilisers and steels and whether it could pose any harm to the employees of a factory. For the manufacture of monolayer BP in large quantities, EELS would be useful for determining the presence of defects which would be detrimental for use in computing.

Further Work and Further Discussion

The EELS can be calculated for the individual WP P4 molecules for comparison with those of monolayer BP in addition to the bulk forms of WP and BP. It is likely that the spectra for monolayer BP would have some resemblance to that of the bulk and individual forms of WP due to the similarities in the electronic properties.

The chemical properties of WP that allow it to be used as fertilisers are difficult to study with DFT without involving the complete chemical and biological mechanisms. However, the metastable nature of WP that might make it difficult to keep can be explored to find ways of preserving the chemical.

It's worth noting that the electronic properties of exfoliated BP can be significantly affected by defects, impurities, and strain, which can result in changes to the bandgap, band structure, and overall electronic properties. The effective electron masses can be extracted for comparison with other conductive monolayers. Theoretical studies have shown that the electronic properties of both allotropes can be engineered by applying strain or incorporating impurities to tailor their properties for specific applications.

As effective masses of charge carriers of BP depend on the direction of charge transfer and also can change significantly by the magnitude and direction of applied strain. The preferred direction (AM or ZZ) for charge carrier transport can be determined. [6]

The properties of monolayer BP should be studied in greater detail in comparison to graphene and tin sulphide (SnS) due to its semiconducting properties for potential use in electronic devices.

Conclusion

In conclusion, both black and WP have unique structural properties that determine their electronic and optical properties, mechanical stability, and potential applications. The structural properties of BP change significantly when exfoliated to single-layer form, while the structural properties of WP are dominated by the properties of the individual P4 molecules. The band gap and electronic properties of bulk BP are also likely to be dependent on the strain that the individual P4 molecules experience.
The calculations were very useful in understanding the basic properties of WP, BP and their individual forms. The next steps are the study the materials in relation to others to understand their applications for new technologies for BP and improvements to current processes for WP.

References

[1] White Phosphorus: Systemic Agent - Center for Disease Control and Prevention

[2] Phosphorus K4 Crystal: A New Stable Allotrope (2016) Liu et al.

[3] Effects of strain on the band gap and effective mass in two-dimensional monolayer GaX (X = S, Se, Te) (2014) Huang et al.

[4] Guo, Zhinan; Zhang, Han; Lu, Shunbin; Wang, Zhiteng; Tang, Siying; Shao, Jundong; Sun, Zhengbo; Xie, Hanhan; Wang, Huaiyu (2015). "From Black Phosphorus to Phosphorene: Basic Solvent Exfoliation, Evolution of Raman Scattering, and Applications to Ultrafast Photonics". Advanced Functional Materials. 25 (45): 6996–7002. doi:10.1002/adfm.201502902. S2CID 49347466.

[5] Liu, Han; Neal, Adam T.; Zhu, Zhen; Luo, Zhe; Xu, Xianfan; Tománek, David; Ye, Peide D. (2014). "Phosphorene: An Unexplored 2D Semiconductor with a High Hole Mobility". ACS Nano. 8 (4): 4033–4041. arXiv:1401.4133. doi:10.1021/nn501226z. PMID 24655084. S2CID 59060829.

[6] Recent advances in synthesis, properties, and applications of phosphorene (2017) Akhtar et al.